J Supercond Nov Magn (2011) 24:1497–1500
DOI 10.1007/s10948-010-0881-y

ORIGINAL PAPER

The Multiferroic Properties of $(Bi_{0.9}Ba_{0.1})(Fe_{0.95}Mn_{0.05})O_3$ Films

Qingyu Xu · Zheng Wen · Jinlong Gao · Xiao Liu · Di Wu · Shaolong Tang · Bin Yang

Received: 30 July 2010 / Accepted: 7 September 2010 / Published online: 22 September 2010

Abstract $(Bi_{0.9}Ba_{0.1})(Fe_{0.95}Mn_{0.05})O_3$ films were prepared on $LaNiO_3$-coated surface oxidized Si substrates. XRD and Raman measurements confirm that the $(Bi_{0.9}Ba_{0.1})(Fe_{0.95}Mn_{0.05})O_3$ film has pure R3c structure. Clear ferromagnetism with saturated magnetization of about 25 emu/cm^3 has been observed at room temperature. The ferroelectric properties of the $(Bi_{0.9}Ba_{0.1})(Fe_{0.95}Mn_{0.05})O_3$ film was confirmed by the observation of the ferroelectric domains and the converse piezoelectric coefficient d_{33} versus applied voltage hysteresis loops by piezoelectric force microscopy (PFM). The observation of ferromagnetism and ferroelectricity in $(Bi_{0.9}Ba_{0.1})(Fe_{0.95}Mn_{0.05})O_3$ films indicates the potential multiferroic applications.

Keywords Multiferroic · $BiFeO_3$ · Ferroelectricity · Ferromagnetism

Q. Xu (✉)
Department of Physics, Southeast University, Nanjing 211189, China
e-mail: xuqingyu@seu.edu.cn

Z. Wen · D. Wu
Department of Materials Science and Engineering, Nanjing University, Nanjing 210008, China

J. Gao · S. Tang
Department of Physics, Nanjing University, Nanjing 210008, China

X. Liu · B. Yang
Center for Condensed Matter Science and Technology, Department of Physics, Harbin Institute of Technology, Harbin 150001, China

1 Introduction

$BiFeO_3$ is one of the most important multiferroic materials because of its high ferroelectric Curie temperature ($T_c \sim 825\,^\circ C$) and antiferromagnetic Néel temperature ($T_N \sim 370\,^\circ C$), which attracts intensive research interests for its potential applications in memories, spintronics and magnetoelectric sensor devices [1]. Though enhanced ferroelectric polarization with remnant polarization P_r of $\sim 60\ \mu C/cm^2$ has been reported in the high-quality epitaxial $BiFeO_3$ films and single crystals [2, 3], the large leakage current of BFO thin films at RT is known to be a serious problem [4]. $BiFeO_3$ has a superimposed incommensurate cycloid spin structure with a periodicity of about 64 nm [5], which cancels the macroscopic magnetization and inhibits the observation of the linear magnetoelectric effect (ME) [6]. Thus, much effort has been made to improve the magnetization and suppress the leakage current in $BiFeO_3$.

Among the various attempts, ion substitution is an effective method, enhanced RT ferromagnetism and low leakage current have been reported [7, 8]. Compared with other ion substitution, Ba substituted the Bi sites and enhanced RT ferromagnetism with saturated magnetization more than 1 emu/g has been reported [7, 9]. Mn has been substituted on Fe sites, and effective suppression of leakage current and improved ferroelectric properties have been reported [8, 10]. Thus, in this paper, we combined the Ba and Mn substitution in $BiFeO_3$, enhanced RT ferromagnetism and improved electrical properties have been observed for the potential multiferroic applications.

2 Experimental Details

$(Bi_{0.9}Ba_{0.1})(Fe_{0.95}Mn_{0.05})O_3$ films were deposited onto $LaNiO_3$-coated surface oxidized Si substrates by chemical

solution deposition. $LaNiO_3$ bottom electrode was first deposited on the surface oxidized Si substrate. $La(NO_3)_3{\cdot}6H_2O$ and $Ni(NO_3)_2{\cdot}6H_2O$ were dissolved in ethylene glycol monomethylether, and deposited onto the substrates by spin coating at 5000 rpm for 30 s. The wet films were dried and pyrolyzed at 160 °C for several minutes in air. These steps were repeated several times to increase film thickness. Then the films are annealed finally at 700 °C for 30 min in air for achieving better crystallinity. The bottom $LaNiO_3$ electrode was confirmed to be highly conductive by the two-point measurement by a multimeter. The $(Bi_{0.9}Ba_{0.1})(Fe_{0.95}Mn_{0.05})O_3$ film was deposited on the $LaNiO_3$ film. The precursor were prepared by dissolving $Bi(NO_3)_3{\cdot}5H_2O$, $Ba(NO_3)_2$, $Fe(NO_3)_3{\cdot}9H_2O$ and $Mn(NO_3)_2$ in acetic acid. Ethylene glycol was added to adjust the viscosity. The same deposition steps as $LaNiO_3$ were followed, and the final annealing was taken at 580 °C for 30 min in air. The X-ray diffraction (XRD) with Cu Kα radiation was used for the phase analysis. The structures of samples were studied by scanning electron microscope (SEM, FEI Quanta200) and scanning probe microscope (SPM, Veeco Nanoscope Dimension V). Raman measurements were carried out on a Horiba Jobin Yvon LabRAM HR 800 micro-Raman spectrometer with 785 nm excitation source under air ambient condition focused over a 1 μm diameter area. The magnetization of $(Bi_{0.9}Ba_{0.1})(Fe_{0.95}Mn_{0.05})O_3$ was measured by a vibrating sample magnetometer (VSM) integrated in a physical property measurement system (PPMS-9, Quantum Design).

3 Results and Discussion

Figure 1 shows the XRD pattern of $(Bi_{0.9}Ba_{0.1})(Fe_{0.95}Mn_{0.05})O_3$ film. Except for the diffraction peaks corresponding to $LaNiO_3$, all the diffraction peaks can be indexed to the rhombohedral perovskite structure (R3c) as $BiFeO_3$. The lattice constants calculated from the XRD pattern are $a = 5.562$ Å and $c = 13.808$ Å. Both a and c are smaller than those of $BiFeO_3$ bulk [11], and this is due to the lattice mismatch between $BiFeO_3$ and $LaNiO_3$, which induces the compressive stress on $(Bi_{0.9}Ba_{0.1})(Fe_{0.95}Mn_{0.05})O_3$ film [12]. Figure 2(a) shows the surface morphology by SEM. The film shows the columnar structure with grain size of about 100 nm and the film is rather dense. Furthermore, some pits can be observed. As shown by the cross-sectional SEM image of the film (Fig. 2(b)), the contrast between $LaNiO_3$ and $(Bi_{0.9}Ba_{0.1})(Fe_{0.95}Mn_{0.05})O_3$ is rather weak. The thickness of $LaNiO_3$ is about 140 nm, and the thickness of $(Bi_{0.9}Ba_{0.1})(Fe_{0.95}Mn_{0.05})O_3$ is about 160 nm.

The Raman spectrum of samples is shown in Fig. 3. Except for the peak at 400 cm^{-1} from $LaNiO_3$ and 520 cm^{-1} from Si [12], the clearly resolved Raman modes can all be indexed to the modes of $BiFeO_3$ molecules with R3c structure [13]. As the intensity of the Raman peaks of $BiFeO_3$ decreases with increasing temperature, not all modes can be clearly observed above RT [14]. Compared with the Raman spectrum of $BiFeO_3$, the peak intensity of the E-9 mode is significantly larger than other modes. A similar phenomenon has been observed in thin $BiFeO_3$ film on $LaNiO_3$ buffer layer, and this can be attributed to

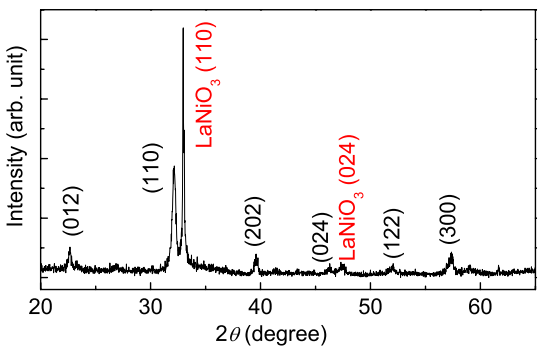

Fig. 1 XRD pattern of $(Bi_{0.9}Ba_{0.1})(Fe_{0.95}Mn_{0.05})O_3$ film

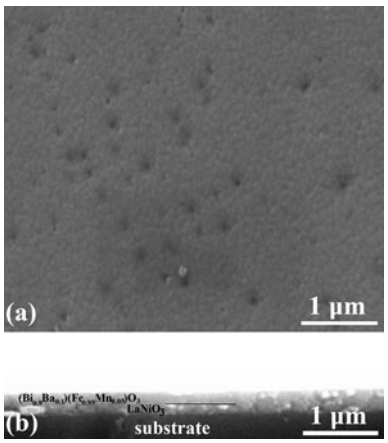

Fig. 2 (**a**) surface morphology image by SEM, (**b**) the cross-sectional SEM image of $(Bi_{0.9}Ba_{0.1})(Fe_{0.95}Mn_{0.05})O_3$ film

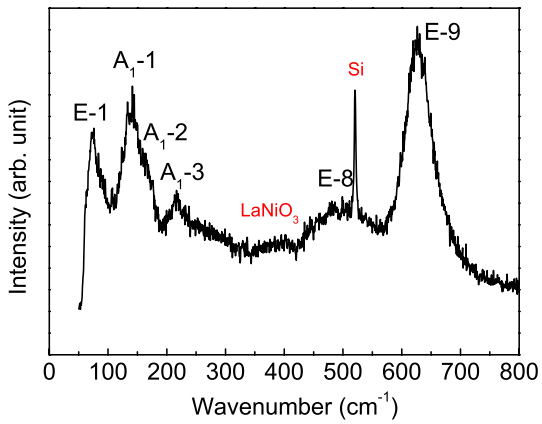

Fig. 3 Raman spectrum of $(Bi_{0.9}Ba_{0.1})(Fe_{0.95}Mn_{0.05})O_3$ film

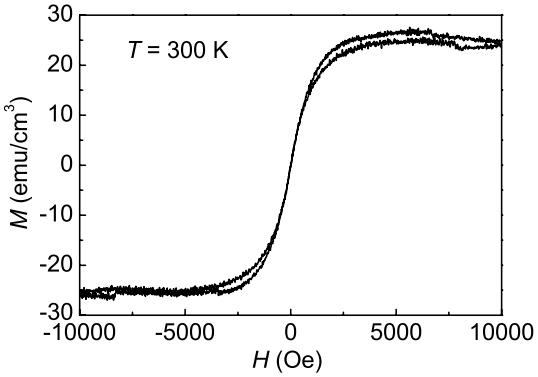

Fig. 4 Magnetic hysteresis loop of $(Bi_{0.9}Ba_{0.1})(Fe_{0.95}Mn_{0.05})O_3$ film measured at 300 K

the compressive strain induced by the mismatch between $(Bi_{0.9}Ba_{0.1})(Fe_{0.95}Mn_{0.05})O_3$ and $LaNiO_3$ lattice [12].

Figure 4 shows the M–H curve measured at 300 K. The clear hysteresis loop indicates the RT ferromagnetism in $(Bi_{0.9}Ba_{0.1})(Fe_{0.95}Mn_{0.05})O_3$ film. The magnetization saturates at about 2500 Oe, and the saturated magnetization of $(Bi_{0.9}Ba_{0.1})(Fe_{0.95}Mn_{0.05})O_3$ film is about 25 emu/cm^3, which equals to be about 3 emu/g with density of 8.25 g/cm^3 for $BiFeO_3$ [15]. The saturated magnetization (25 emu/cm^3) of $(Bi_{0.9}Ba_{0.1})(Fe_{0.95}Mn_{0.05})O_3$ film is much larger than that of $BiFeO_3$ film with similar thickness (<5.3 emu/cm^3) prepared by the same method [12, 16]. We attribute the enhanced magnetization mainly to the substitution of Ba ions, which have larger ionic radius [9], because no significant enhancement of magnetization has been obtained by the Mn doping [10, 11]. The saturated magnetization is significantly larger than that of bulk Ba substituted $BiFeO_3$ [7, 9]. This might be due to the compressive strain induced by the lattice mismatch of the $LaNiO_3$ buffer layer, as similar phenomenon of enhanced magnetization has been observed in $BiFeO_3$ thin film [12]. The film exhibits a soft ferromagnetic property, the coercivity is much smaller than that of the bulk Ba substituted $BiFeO_3$ [7, 9].

The ferroelectric behavior of $(Bi_{0.9}Ba_{0.1})(Fe_{0.95}Mn_{0.05})O_3$ film was studied through piezoelectric force microscopy (PFM) in the SPM system. A comparison of simultaneously acquired topography and out-of-plane PFM images are shown in Fig. 5. Similar to the previous study [17], the weak contrast of the ferroelectric domains are associated with grains in our polycrystalline film. The tendency to form a single domain pattern also favors the improvement of ferroelectricity [17]. The pits observed by SEM can be clearly observed in the topography image, and the deepness of the pits is up to about 25 nm. However, these pits are not the ferroelectric dead regions. For example, the pits indicated by the arrows, clear positive piezoelectric force response has been observed. Thus it is suggested that the ferroelectric properties of $(Bi_{0.9}Ba_{0.1})(Fe_{0.95}Mn_{0.05})O_3$ film by further optimizing our film deposition process to get a smoother film surface.

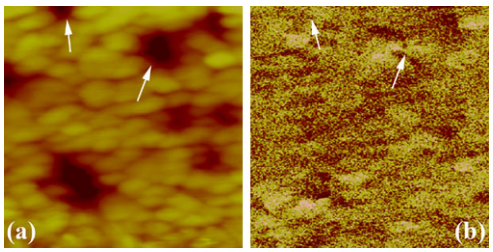

Fig. 5 (**a**) AFM, (**b**) PFM image $(Bi_{0.9}Ba_{0.1})(Fe_{0.95}Mn_{0.05})O_3$ film with an area of 1×1 μm^2

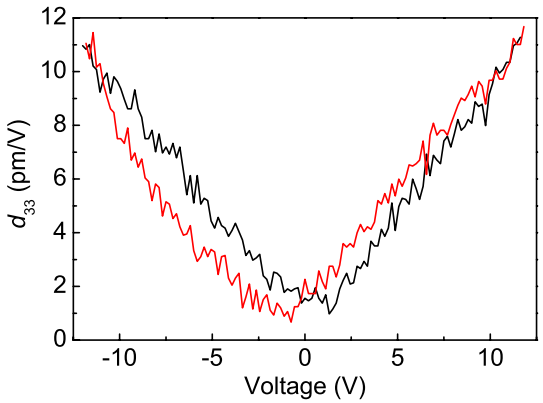

Fig. 6 The d_{33} versus applied voltage hysteresis loop of $(Bi_{0.9}Ba_{0.1})(Fe_{0.95}Mn_{0.05})O_3$ film

The converse piezoelectric coefficient d_{33} versus applied voltage hysteresis loop is plotted in Fig. 6 by randomly selecting a point on the film surface. The d_{33} value is about 11 pm/V with the highest voltage of 12 V. This value is comparable to the La-doped $BiFeO_3$ film [17]. In $BiFeO_3$ film prepared by the same method, only constant piezoelectric coefficient in the applied voltage range has been found [18]. The observation of the hysteresis loop of d_{33} in dependence on the applied voltage indicates the improved ferroelectricity in $(Bi_{0.9}Ba_{0.1})(Fe_{0.95}Mn_{0.05})O_3$ film [19].

The leakage mechanism was studied by the electric field (E) dependent leakage current (J). Figure 7 shows the J vs. E characteristics measured at RT in logarithmic scale. It should be noted that the $(Bi_{0.9}Ba_{0.1})(Fe_{0.95}Mn_{0.05})O_3$ film is easily broken down when applying high voltage, which might be due to the pits on the film surface. To understand the leakage mechanism, we concentrate on the J–E curve below the broken-down field. The leakage current at RT is close to 10^{-3} A/cm^2 under low electrical field, which is about one order lower than the reported leakage current (10^{-2} A/cm^2) of the annealed $BiFeO_3$ film with low O vacancies [20], and can be attributed to the Mn substitution [8]. As can be seen, in the higher electric field range, the plot of log J and log E is linear and the slope is around 2,

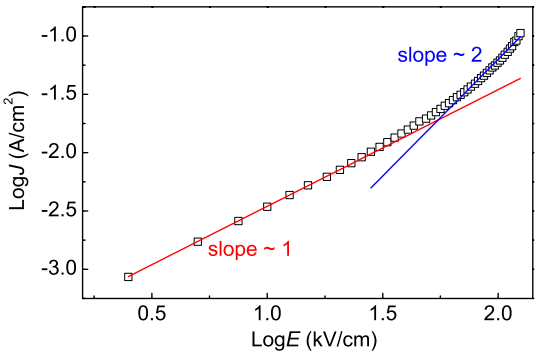

Fig. 7 $\log J$ versus $\log E$ characteristics of $(Bi_{0.9}Ba_{0.1})(Fe_{0.95}Mn_{0.05})O_3$ film at positive bias

in agreement with the space-charge-limited current (SCLC) behavior [20]. At lower electric field, the $\log J$ and $\log E$ is also linear with slope of around 1, which is attributed to the Ohmic contact. In contrast to the abrupt change of slope [20], the slope increases gradually from 1 to 2, which can be modeled by the modified Child's law ($J \propto E^{\alpha}, \alpha > 1$), and can be explained by the filling of the deep traps formed by the doped Mn ions called the trap-filled-limit region [4]. The reduction of the leakage current is due to the formation of deep traps by the Mn substitution in $BiFeO_3$ [4].

4 Conclusions

In conclusion, $(Bi_{0.9}Ba_{0.1})(Fe_{0.95}Mn_{0.05})O_3$ films were prepared on the $LaNiO_3$-coated surface oxidized Si substrate. The XRD and Raman measurements confirm the R3c structure of the film. Clear RT ferromagnetism has been observed. The ferroelectric domains and the converse piezoelectric coefficient d_{33} versus applied voltage hysteresis loops observed by piezoelectric force microscopy (PFM) confirm the ferroelectric properties. Our results clearly demonstrate that ion codoping is an effective strategy to both improve the ferromagnetism and ferroelectricity of $BiFeO_3$ for the multiferroic applications.

Acknowledgements This work is supported by the National Natural Science Foundation of China (50802041, 50872050), National Key Projects for Basic Researches of China (2010CB923404, 2009CB-929503), by NCET-09-0296 and Southeast University.

References

1. Catalan, G., Scott, J.F.: Adv. Mater. **21**, 2463 (2009)
2. Wang, J., Neaton, J.B., Zheng, H., Nagarajan, V., Ogale, S.B., Liu, B., Viehland, D., Vaithyanathan, V., Schlom, D.G., Waghmare, U.V., Spaldin, N.A., Rabe, K.M., Wuttig, M., Ramesh, R.: Science **299**, 1719 (2003)
3. Lebeugle, D., Colson, D., Forget, A., Viret, M., Bonville, P., Marucco, J.F., Fusil, S.: Phys. Rev. B **76**, 024116 (2007)
4. Kawae, T., Terauchi, Y., Tsuda, H., Kumeda, M., Morimoto, A.: Appl. Phys. Lett. **94**, 112904 (2009)
5. Lebeugle, D., Colson, D., Forget, A., Viret, M., Bataille, A.M., Gukasov, A.: Phys. Rev. Lett. **100**, 227602 (2008)
6. Béa, H., Bibes, M., Petit, S., Kreisel, J., Barthélémy, A.: Philos. Mag. Lett. **87**, 165 (2007)
7. Naik, V.B., Mahendiran, R.: Solid State Commun. **149**, 754 (2009)
8. Allibe, J., Infante, I.C., Fusil, S., Bouzehouane, K., Jacquet, E., Deranlot, C., Bibes, M., Barthélémy, A.: Appl. Phys. Lett. **95**, 182503 (2009)
9. Khomchenko, V.A., Kiselev, D.A., Kopcewicz, M., Maglione, M., Shvartsman, V.V., Borisov, P., Kleemann, W., Lopes, A.M.L., Pogorelov, Y.G., Araujo, J.P., Rubinger, R.M., Sobolev, N.A., Vieira, J.M., Kholkin, A.L.: J. Magn. Magn. Mater. **321**, 1692 (2009)
10. Huang, J., Wang, Y., Lin, Y., Li, M., Nan, C.W.: J. Appl. Phys. **106**, 063911 (2009)
11. Zheng, X., Xu, Q., Wen, Z., Lang, X., Wu, D., Qiu, T., Xu, M.X.: J. Alloys Compd. **499**, 108 (2010)
12. Wang, Y., Lin, Y., Nan, C.: J. Appl. Phys. **104**, 123912 (2008)
13. Yang, Y., Sun, J.Y., Zhu, K., Liu, Y.L., Wan, L.: J. Appl. Phys. **103**, 093532 (2008)
14. Rout, D., Moon, K., Kang, S.L.: J. Raman Spectrosc. **40**, 618 (2009)
15. Taussig, A.R.: Growth and characterization of bismuth perovskite thin films for integrated magneto-optical isolator applications. Master thesis, Harvard University, 2007, p. 55
16. Naganuma, H., Okamura, S.: J. Appl. Phys. **101**, 09M103 (2007)
17. Wang, Y., Nan, C.: J. Appl. Phys. **103**, 114104 (2008)
18. Iakovlev, S., Solterbeck, C.-H., Kuhnke, M., Es-Souni, M.: J. Appl. Phys. **97**, 094901 (2005)
19. Yang, Y.C., Song, C., Wang, X.H., Zeng, F., Pan, F.: J. Appl. Phys. **103**, 074107 (2008)
20. Yang, H., Wang, Y.Q., Wang, H., Jia, Q.X.: Appl. Phys. Lett. **96**, 012909 (2010)